Kinetics of Block Copolymer Adsorption on Dielectric Surfaces from a Selective Solvent

Mark R. Munch and Alice P. Gast*

Department of Chemical Engineering, Stanford University, Stanford, California 94305.
Received July 5, 1989; Revised Manuscript Received November 1, 1989

ABSTRACT: We present measurements of the adsorption of poly(ethylene oxide)/polystyrene block copolymers on dielectric surfaces from gently flowing solutions of cyclopentane. We observe that micellization has a drastic effect on the adsorption. Above the cmc, the rapid initial rate of adsorption indicates that micelles adsorb. We show the first results of the time evolution of the surface concentration, thickness, and refractive index of adsorbing block copolymers, giving insight into the mechanisms of the layer formation. Experiments on two block copolymer samples having small anchor blocks and large tails demonstrate the dependence of the surface density and thickness on tail size.

Introduction

Much recent attention has been directed toward describing the adsorption of block copolymers from solution.[1-7] In a selective solvent, block copolymers adsorb in a conformation such that the block interacting unfavorably with the solvent adsorbs to the surface, leaving the solvated block extended away from the surface. The block binding to the surface is commonly referred to as the anchor block, or head, while the solvated block is called the tail. The same thermodynamic factors driving the adsorption cause block copolymers to aggregate into structures such as micelles or lamellae.[1,2] These aggregates may change the chemical potential of the solution, thereby affecting the adsorption.[1,2] The majority of the work to date comprises theoretical investigations describing the adsorbed layer properties such as the layer thickness, surface density, and concentration profile within the layer as a function of molecular weight, composition, and solvency.[1-4] Adsorbed block copolymers have been described as terminally attached chains in which the surface density is solely determined by the size of the anchor block.[4] However, when the anchor group is small compared to the tail, the repulsion between tails may govern their surface density.[5] Equilibrium models show that the surface density, obtained from a minimization of the free energy, is in general governed by the repulsion between the tails as well as the packing of the anchoring block.[1-3]

There have been fewer experimental studies of block copolymer adsorption. Most of these were carried out on the surface force apparatus.[4,6,7] These studies have confirmed that the adsorbed layers formed by block copolymers are highly extended up to 6 times the radius of gyration. This technique has enabled researchers to investigate the thickness of the layer as a function of molecular weight; the layer thickness scales with the molecular weight to a power ranging from 0.7 to 1.0, depending on the composition.[4,6] In the extreme composition limit of one anchor unit, such as end-functionalized polystyrene, Taunton et al.[8] found that the thickness scales with the molecular weight to the 0.6 power. They found that this lower scaling exponent was due to an increase in the mean anchor spacing as the size of the tail increased. In this case, the surface density of the chains is determined by repulsions between the tails. It is important to consider both the anchor block and the tails when predicting the surface density of adsorbed diblock copolymer layers. The results indicate that, for larger anchoring blocks, the surface density is determined by the anchor group, resulting in a linear dependence on molecular weight. However, when the anchor is small relative to the tail, repulsions between the bulky tails become important and influence the surface density, resulting in a weaker dependence.[2,3,5] The most recent results on adsorbed diblock copolymers come from a study of hindered convective transport in capillary-like pores by Webber and co-workers.[9] Their data also suggest that the surface density depends on both the tail and anchor size. The experiments mentioned above are all equilibrium measurements.

Table I
Polymer Characteristics

sample	M_w	M_w/M_n	PEO, wt %	N_{PS}	N_{PEO}
P170/1730	1.87×10^5	1.10	4	1730	170
P83/3470	3.65×10^5	1.14	1	3470	83
PS	1.6×10^5	1.10			

In a previous paper,[10] we presented the first results on the dynamics of block copolymer adsorption from flowing solutions. We are interested in how block copolymers form very thick layers at high surface densities and therefore focus on the adsorption kinetics to elucidate the mechanisms of this process. In this paper we present results demonstrating that aggregation of block copolymers affects the kinetics and final adsorbed amount. We explain these kinetic results with the steady-state solution of the convective diffusion equation. We observe the development of the average thickness and refractive index as the surface concentration develops with time and compare the layer thicknesses and surface densities of two block copolymer samples. Both copolymers consist of a small, insoluble, anchor block of poly(ethylene oxide), and a large, soluble polystyrene tail, providing us with a model system to study the effects of tail size.

Experimental Section

We purchased two low polydispersity copolymers of poly(ethylene oxide)/polystyrene, PEO/PS, from Polymer Laboratories, Inc. We also investigated homopolymer polystyrene, obtained from Polysciences, Inc. The polymer characteristics are given in Table I. We refer to the copolymer samples as P170/1730 and P83/3470, respectively, denoting the number, N, of PEO and PS segments. The number of polystyrene segments is much larger than the number of PEO segments, with ratios being 10:1 and 40:1, respectively. We chose cyclopentane as the solvent since at the temperature of 23 °C in this study, it is a selective solvent for polystyrene, with its θ point at 19.5 °C, and a nonsolvent for poly(ethylene oxide).[11] Cyclopentane, 95% purity, obtained from Aldrich Chemical Co., contains up to 5% noncyclic pentanes. Cyclopentane has a low refractive index, n_2 =

0024-9297/90/2223-2313$02.50/0

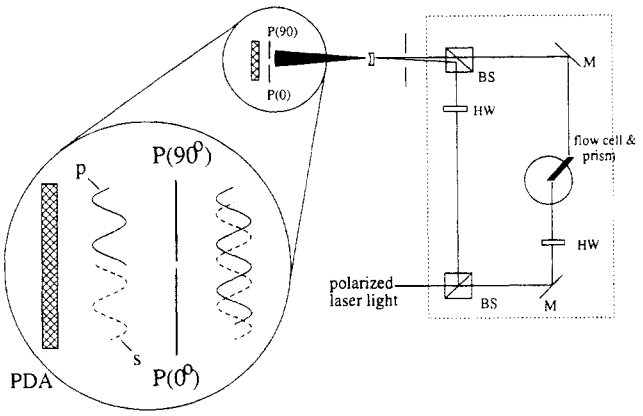

Figure 1. Schematic of the experimental apparatus to measure the phase changes for the two polarizations simultaneously. The following elements comprise the interferometer: the lower BS is a variable attenuator beam splitter, M's are mirrors, HW are half-wave plates, the upper BS is a cube beam splitter, PDA is the photodiode array, and P's are polarizers.

1.408, and therefore a relatively high specific refractive index increment with polystyrene of 0.196 mL/g.[11] The critical micelle concentration of P170/1730 was between 1×10^{-4} and 2×10^{-4} g/mL as determined by dynamic light scattering. No critical micelle concentration was detected for P83/3470 up to a concentration of 1.75×10^{-4} g/mL; thus, no micelles are present in experiments with this copolymer. The adsorption studies are performed under mild flow conditions to minimize diffusion-controlling processes. A Fluid Metering, Inc., pump with a low-flow pulse dampener is used to pump the solutions down both sides of the reflection prism. The flow chamber on each side of the prism has dimensions (l = 40.72 mm) × (w = 14.17 mm) × (b = 1.40 mm). In this system, the wall shear rate, γ, can be varied from 2.7 to 32.5 s^{-1}. All experiments were performed at a wall shear rate of 15 s^{-1} except when the flow rate was explicitly varied.

We are particularly interested in studying adsorption onto dielectric materials because their surfaces are of lower energy and thus more selective than the high energy surfaces of metals. Polymers are known to adsorb readily onto metals, even from good solvents. We have selected glass and sapphire as our substrates. We use a method presented previously,[10] employing multiple total internal reflections through glass and sapphire prisms. Light undergoing total internal reflection at an interface experiences a phase change that is a function of the refractive index and thickness of a layer at the interface. The dependence of the phase change on refractive index and thickness is different for the two principal, orthogonal polarization states of light, parallel and perpendicular to the plane of incidence. In order to obtain the average thickness and refractive index of the layer, we simultaneously measure the changes in phase for both polarization states.

A modified Mach–Zehnder interferometer allows us to independently measure the phase changes of the two polarizations as shown in Figure 1. Linearly polarized light, λ = 514.5 nm, from a frequency-stabilized, argon ion laser is split into the two arms of the interferometer by a variable-attenuator beam splitter. The light in each arm is rotated 45° by half-wave plates to sample both polarizations, 0° and 90°, with an equal intensity of light. A mirror directs one beam into the reflection plate where it undergoes multiple total internal reflections. A second beam splitter is used to combine the beam of interest at a small angle with the reference, also linearly polarized at 45°, to produce an interference pattern for each polarization. The interference patterns are projected onto a Reticon 1024 element photodiode array by a diverging lens. Two polarizers, oriented at 0° and 90°, mounted in front of the photodiode array separate the interference patterns. We measure the phase change of the light for each polarization by monitoring the fringe positions at the photodiode array. We view the fringes on a digitizing oscilloscope and record their positions every second, storing the data on a computer.

Our first adsorption substrate was a sapphire parallelepiped,[10] 50 mm × 20 mm × 1 mm, with a wedge angle of 60°. We chose sapphire to verify our final surface coverage and initial cleanliness of the prism with an ATR/FTIR spectrometer. With this prism we were able to obtain surface concentration as a function of time but could not independently determine the refractive index and thickness because only one polarization can be used since sapphire is birefringent. Having confirmed our procedure with IR analysis, we changed to a glass parallelepiped, 50 mm × 20 mm × 1.651 mm, with a wedge angle of 51° designed to minimize the reflection at the prism entrance. With glass having no birefringence, it is possible to simultaneously measure the refractive index and thickness. The number of reflections sampling the interface, typically 20–30, is given by $N_R = (l/h) \tan \theta_0$, where h is the prism thickness, l is the flow chamber length, and θ_0 is the angle of incidence.

As mentioned above, we measure the phase changes, δ_s and δ_p, as copolymer adsorbs to the surface of the substrate. Here the s and p subscripts denote polarizations of light parallel and perpendicular to the plane of incidence, respectively. From this pair of phase changes we compute the adsorbed layer's average refractive index, n, and average thickness, d, from the following relations derived from the Fresnel equations.[12] For an angle of incidence slightly greater than the critical angle for total internal reflection, the phase changes for a single reflection are given by

$$\tan \delta_m = \frac{(r_{01m}^2 - 1) \sin (x - \delta_{12m})}{2r_{01m} + (1 + r_{01m}^2) \cos (x - \delta_{12m})} \quad (1)$$

where m denotes the s or p polarization and

$$x = (4\pi n_1 d/\lambda) \cos \theta_1$$

$$\delta_{12s} = 2 \tan^{-1} \left(\frac{(n_1^2 \sin \theta_1^2 - n_2^2)^{1/2}}{n_1 \cos \theta_1} \right)$$

$$\delta_{12p} = 2 \tan^{-1} ((n_1^2/n_2^2) \tan (\delta_{12s}/2))$$

$$\theta_1 = \sin^{-1} ((n_0/n_1) \sin \theta_0)$$

and the r_{01s} and r_{01p} are the Fresnel coefficients for reflection for the prism–film (0–1) interface, λ is the wavelength of light, n_1 is the refractive index of the film, n_2 is the refractive index of the solution, and θ_1 is the angle of refraction in the film (medium 1). The phase differences measured in an experiment are those given by eq 1 relative to the case where d = 0 and $n_1 = n_2$. Therefore, by measuring the phase changes, δ_p and δ_s, we measure the average refractive index, n_1, and thickness, d, of the adsorbed layer. We interpret this thickness based on another, more realistic concentration profile in the Appendix.

The surface concentration of adsorbed polymer is given by

$$C_s = \frac{(n_1 - n_2)d}{dn/dc} = \frac{\Delta n d}{dn/dc} \quad (2)$$

where dn/dc is the specific refractive index increment for the polymer–solvent system and Δn is the film index, n_1, minus the solution index, n_2. Our block copolymer solutions have a specific refractive index increment of 0.196 mL/g, approximately equal to that of polystyrene in cyclopentane.

Results

We investigated the adsorption of polystyrene homopolymer on glass and sapphire and found that it does not adsorb from cyclopentane while both block copolymer samples adsorb considerably. In this section we present the results for the adsorption of P170/1730 on glass above and below the critical micelle concentration and find the same kinetic behavior as observed for the adsorption of the same copolymer on sapphire. We present the first results of the time evolution of surface concentration, thickness, and refractive index for adsorbing block copolymers. We then present the adsorption behavior of a copolymer having a different composition, P83/3470.

Adsorption of Homopolymer Polystyrene. We investigated the adsorption of homopolymer polystyrene, M_w

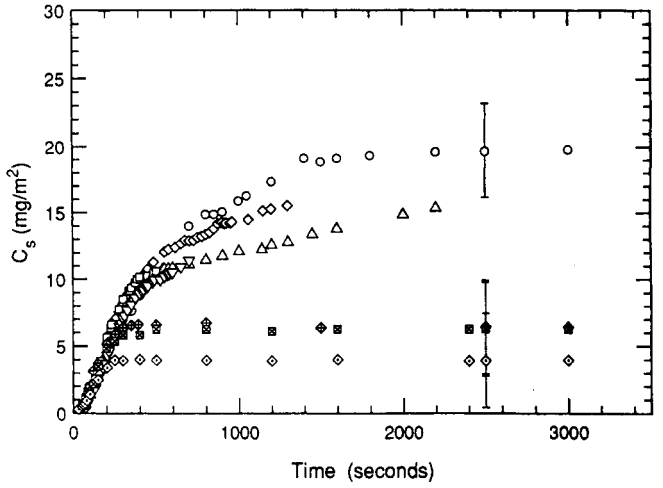

Figure 2. Evolution of the surface concentration as a function of time for adsorption of P170/1730 on glass. The upper set of curves are for bulk copolymer concentrations, $c_0 = (9.6 \pm 0.3) \times 10^{-5}$ g/mL, below the cmc (○, △, ▽, ◇, □). The lower set of curves are for bulk copolymer concentrations above cmc starting with the lowest curve, $c_0 = 2.3 \times 10^{-4}$ g/mL (◈), $c_0 = 3.8 \times 10^{-4}$ g/mL (⊠), and $c_0 = 4.2 \times 10^{-4}$ g/mL (⊕). The wall shear rate is 15 s^{-1}.

= 160 000, on glass from a solution of bulk concentration, $c_0 = 1.0 \times 10^{-4}$ g/mL. As with sapphire, we found no adsorption of polystyrene, indicating that the copolymers adsorb via the poly(ethylene oxide) block. The PEO block binds to the glass surface while the polystyrene block extends into solution.

Adsorption of Poly(ethylene oxide)/Polystyrene P170/1730. We show the time evolution of the surface concentration of P170/1730 on glass for solutions above and below the critical micelle concentration in Figure 2. As mentioned above, the critical micelle concentration for this polymer is in the range 1×10^{-4}–2×10^{-4} g/mL. The lower group of curves in Figure 2 shows adsorption above the cmc while the upper group shows the evolution just below the cmc. The adsorption proceeds initially at a constant rate followed by a decline in the rate at longer times as the surface is covered. Above the cmc, the initial rate of adsorption is faster than that just below cmc as also observed on sapphire[10] and silvered glass.[13] The time required to saturate the surface is about 5 min for adsorption from micellar solutions compared to about 20 min for adsorption from solutions with no micelles. The error bars shown in the figure represent the variation in the final adsorbed amount for experiments repeated at the same conditions.

Figures 2 and 3 also illustrate the differences in the final adsorbed amount above and below the cmc. We see that the final surface concentration is greater for adsorption from solutions just below the cmc than from solutions above the cmc, a result also found on sapphire. This result was verified on sapphire using ATR/FTIR spectroscopy using the aromatic C–H stretch absorbance peak. To quantify ATR measurements, one needs to choose a reference. With a final surface concentration of 11 mg/m^2 on sapphire obtained from a solution of bulk concentration $c_0 = 3.9 \times 10^{-5}$ g/mL as the reference, the final adsorbed amount determined from ATR measurements on sapphire from solutions of $c_0 = 8.3 \times 10^{-5}$ and 5.5×10^{-4} g/mL were $C_{s,f} = 16.2$ and 8.4 mg/m^2, respectively. These ATR values are within experimental error with those measured in the interferometer for solutions above and below the cmc shown by the filled circles in Figure 3. Since we find no measurable difference between the final surface concentrations on sapphire and glass, we combined these results for comparison in Figure 3.

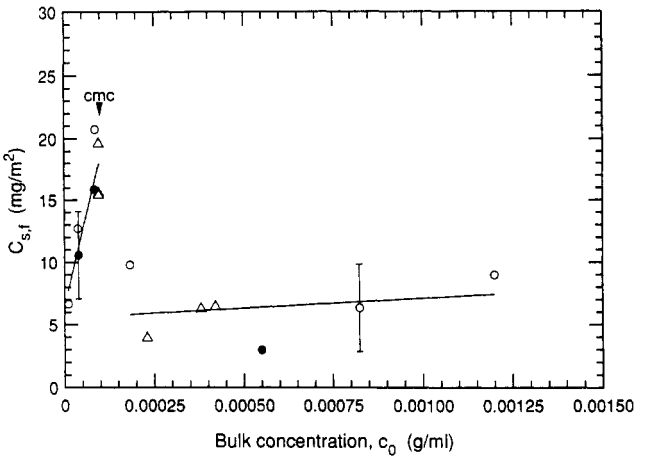

Figure 3. Final adsorbed surface concentration, $C_{s,f}$, of P170/1730 in milligrams per square meter as a function of bulk copolymer concentration, c_0, in grams per milliliter on glass (△) and sapphire (○, ●). The filled circles represent experiments where ATR measurements were performed. The region of the critical micelle concentration is marked. The wall shear rate is 15 s^{-1}.

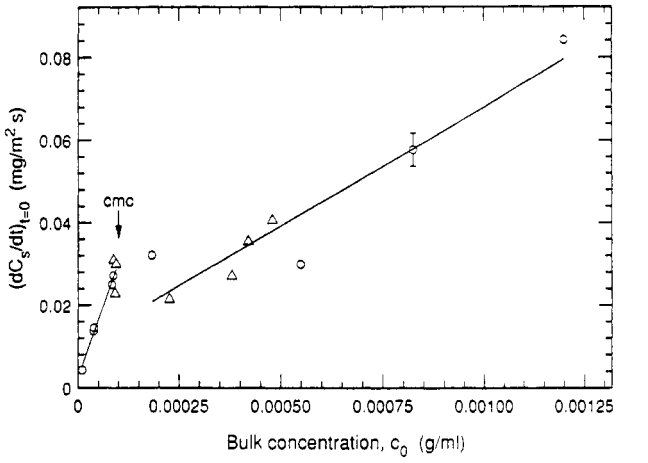

Figure 4. Initial rate of adsorption of P170/1730 on glass (△) and sapphire (○) as a function of bulk copolymer concentration, c_0. The region of the critical micelle concentration is marked. The lines are least-squares fits to the data with slopes having the ratio of 4.85:1. The conditions are the same as in Figure 3.

In Figure 4 we demonstrate the variation of the initial rate of adsorption with bulk copolymer concentration over the entire range of concentrations studied on glass and sapphire. Here we combined the results for glass and sapphire surfaces since there are no observable differences in the adsorption between these surfaces. We find that the initial rate of adsorption varies linearly with the overall copolymer concentration above and below the cmc, with a weaker dependence above the cmc. This difference in dependence on the overall copolymer concentration suggests two adsorption mechanisms, adsorption of single chains below the cmc and adsorption of micelles above the cmc. If adsorption only occurred from single chains at all concentrations, then the initial rate of adsorption would be independent of the bulk concentration above the cmc.

We can compare the adsorption mechanisms above and below the cmc by taking the ratio of the slopes of the lines in Figure 4. A least-squares regression provides 4.85:1. To explain this difference, we consider the transport-limited adsorption of both single chains and micelles in a fully developed, laminar flow. The initial rate of adsorp-

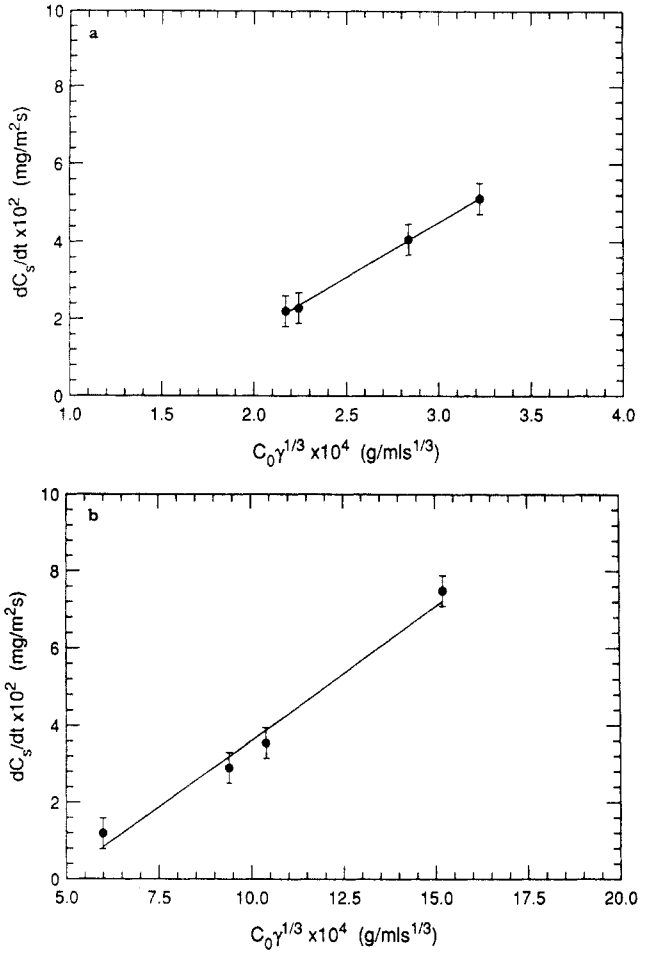

Figure 5. (a) Initial rate of adsorption of P170/1730 on glass as a function of the wall shear rate to the 1/3 power for concentrations just below the cmc, $c_0 = (9.6 \pm 0.5) \times 10^{-5}$ g/mL. (b) Initial rate of adsorption of P170/1730 on glass as a function of the wall shear rate to the 1/3 power for concentrations just above the cmc, $c_0 = (4.8 \pm 0.5) \times 10^{-4}$ g/mL.

tion for this situation is given by Lévêque[14,15]

$$\frac{dC_s}{dt} = \frac{1}{\Gamma(4/3)9^{1/3}}\left(\frac{\gamma}{Dx}\right)^{1/3} Dc_0 \qquad (3)$$

where D is the diffusion coefficient of the diffusing entity, C_0 is its overall concentration, γ is the wall shear rate, Γ is the gamma function, and x is the point of observation. Dividing eq 3 applied to the adsorption of single chains by the same equation applied to the adsorption of micelles predicts that the ratio of the slopes of the two lines in Figure 4 is given by $D_s^{2/3}:D_m^{2/3}$ where D_s and D_m are the diffusion coefficients of the single chains and micelles, respectively. Using diffusion coefficients from dynamic light scattering measurements, we calculate a ratio of 2.5:1, in qualitative agreement with experimental slopes having a ratio of 4.85:1.

The Lévêque solution shows that the initial rate of adsorption depends on the wall shear rate to the 1/3 power. Therefore, we investigated this dependence above and below the cmc at a series of concentrations within $9.6 \pm 0.5) \times 10^{-5}$ and $(4.8 \pm 0.5) \times 10^{-4}$ g/mL, respectively. Parts a and b of Figure 5 demonstrate this dependence on the wall shear rate, suggesting transport-limited adsorption above and below the cmc at these flow rates. If the adsorption were limited by kinetics, there would be no dependence of the adsorption rate on the flow. The intercepts of these curves do not pass through zero, and the slopes are only of the same order of magnitude as those predicted by eq 3, possibly indicating nonideal flow in the cell or other kinetic processes.

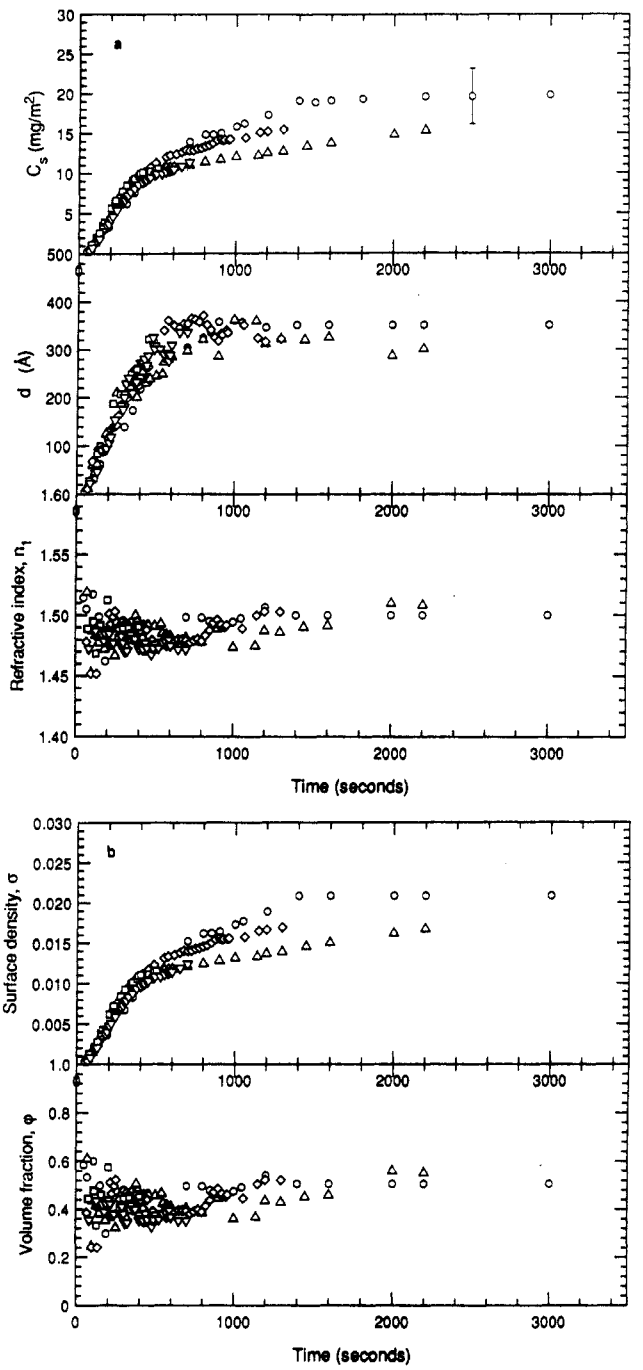

Figure 6. (a) Evolution of the surface concentration, C_s, average thickness, d, and the average refractive index, n_1, of P170/1730 on glass at concentrations of $c_0 = (9.6 \pm 0.3) \times 10^{-5}$ g/mL and a shear rate of 15 s^{-1}. (b) Evolution of the surface density, σ, and the volume fraction, ϕ, in the layer with time for P170/1730. The conditions are the same as in Figure 6a.

Measurement of the phase shifts for two polarizations simultaneously allows the determination of the average refractive index and thickness of the adsorbed layer as mentioned above. The time evolution of the surface concentration, thickness, and refractive index of an adsorbed layer on glass for solutions of P170/1730 at $c_0 = 9.6 \times 10^{-5}$ g/mL are presented Figure 6a. The layer thickness, d, develops as the surface concentration establishes with time. The layer thickens from 0 to 340 Å in the first 15 min and then levels off. The average refractive index of this layer remains relatively constant at $n_1 = 1.49$. At early times, when the phase shifts are small due to the presence of a thin adsorbed film, the refractive index is very sensitive to small changes in the phase

shifts. This sensitivity of n_1 leads to the scatter in the refractive index at small times. The surface concentration appears to increase by stretching the adsorbed chains while maintaining a constant volume fraction in the layer. This is evident in the bottom of Figure 6b where the average volume fraction of the layer is calculated from the average refractive index of the film, n_1, the refractive index of polystyrene, $n_{PS} = 1.59$,[16] and the refractive index of cyclopentane, $n_2 = 1.408$, by

$$\phi = (n_1 - n_2)/(n_{PS} - n_2) \quad (4)$$

The average volume fraction of the adsorbed layer quickly reaches its final constant value of about $\phi = 0.46$. This volume fraction should be consistent with

$$a = (dM_0\phi/C_S N_{Av})^{1/3} \quad (5)$$

defining the segment length a, where $M_0 = 104$ is the monomer molecular weight of polystyrene, N_{Av} is Avogadro's number, and C_s is the surface concentration calculated from eq 2. From the volume fraction for each point in Figure 6b and eq 5, we calculate a segment length a of 5.7 Å. This agrees closely with 5.5 Å obtained from the density of polystyrene, 1.06 g/cm^3, and the monomer molecular weight of 104 and with 5.5 Å calculated previously from the characteristic ratio for poly(*tert*-butylstyrene), $C_\infty = 13.2$.[17] Using this segment length, $a = 5.7$ Å, we calculate a dimensionless surface density from

$$\sigma = \frac{C_s N_{Av} a^2}{M_0 N} \quad (6)$$

where N is the number of polystyrene segments. The surface density is defined such that the surface area per chain is a^2/σ. We see in Figure 6b that the surface density increases with time from 0 to approximately 0.018, or, equivalently, the area per chain decreases to 1800 Å^2. Therefore, as the surface concentration, C_s, develops with time, the surface density, σ, and thickness, d, of the layer increase, while the average volume fraction, ϕ, remains constant.

Adsorption of Poly(ethylene oxide)/Polystyrene P83/3470. We also investigated the time evolution of the surface concentration, thickness, and refractive index of adsorbed layers of P83/3470 on glass from solutions having bulk concentrations around 1.0×10^{-4} g/mL. This block copolymer, having a very small anchor block, half the size of the previous copolymer and a tail twice as large, adsorbs onto glass in a similar manner to P170/1730 as shown in Figure 7a. This copolymer adsorbs with an initial rate of 2.1×10^{-2} mg/m^2·s, 1.24 times slower than the initial rate of 2.6×10^{-2} mg/m^2·s for the same concentration of P170/1730. The prediction from the Lévêque solution for transport-limited adsorption gives an initial rate for P83/3470 that is 1.2 times slower than that for P170/1730, suggesting transport limitations for the adsorption of P83/3470.

Similarly, the layer thickens as the surface concentration increases while the refractive index remains constant at $n_1 = 1.45$. The thickness increases from 0 to 510 Å in approximately 15 min. This adsorbed layer is about 1.5 times that of P170/1730 in Figure 6a. Again, we can convert the refractive index of the layer to volume fraction using the refractive indices of polystyrene and cyclopentane. The average volume fraction of the layer is constant with time at $\phi = 0.24$ as shown in Figure 7b. As before, the segment size, $a = 5.7$ Å, is consistent with other measures. From this value for a and eq 6, we present the dimensionless surface density of the adsorbed layer in Figure 7b. The surface density resembles the surface concentration and increases from 0 to 0.005, 4 times lower than that seen in Figure 6b. A surface density of 0.005 corresponds to an area per chain of 5700 Å^2. Therefore, the surface density and thickness increase with time resembling the surface concentration, while the average volume fraction of the layer remains fairly constant.

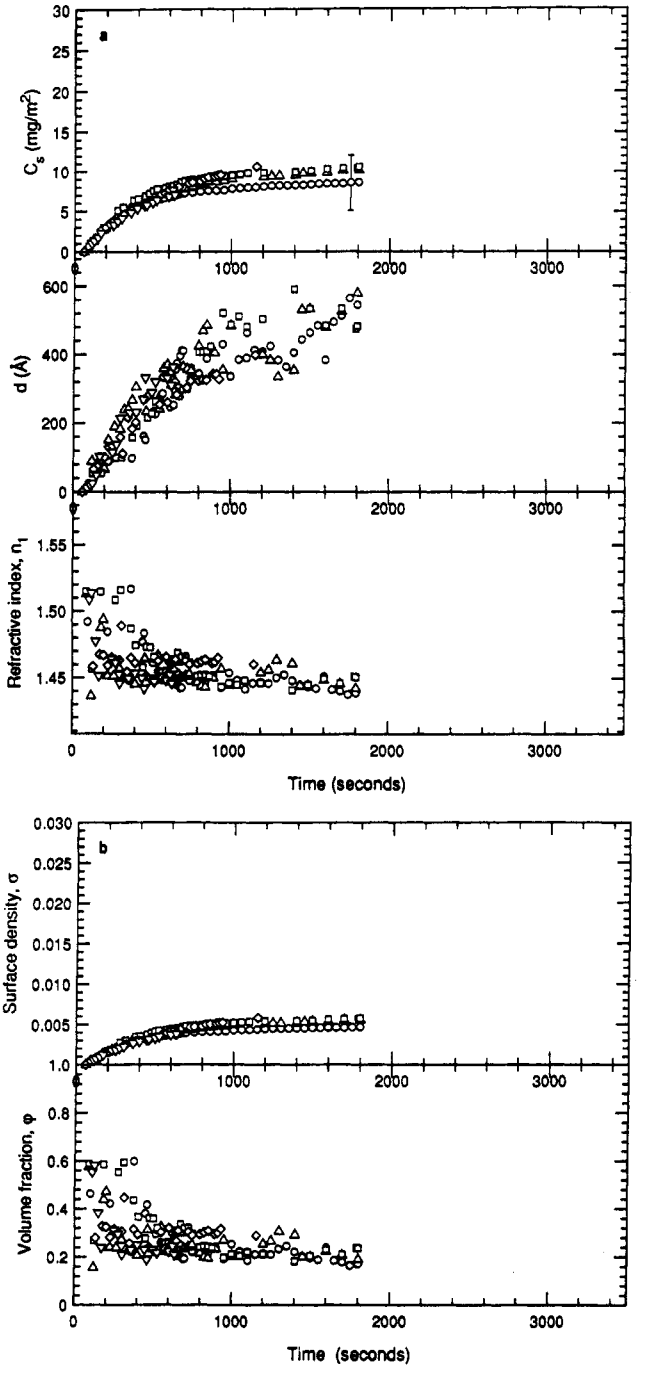

Figure 7. (a) Evolution of the surface concentration, C_s, average thickness, d, and the average refractive index, n_1, of P83/3470 on glass at concentrations of $c_0 = (1.0 \pm 0.3) \times 10^{-4}$ g/mL and a shear rate of 15 s^{-1}. (b) Evolution of the surface density, σ, and the volume fraction, ϕ, in the layer with time for P83/3470. The conditions are the same as in Figure 7a.

Discussion

We find that both of the PEO/PS copolymer samples adsorb on glass from cyclopentane while polystyrene homopolymer does not. Therefore, both block copolymers must adsorb with the PEO block bound to the glass

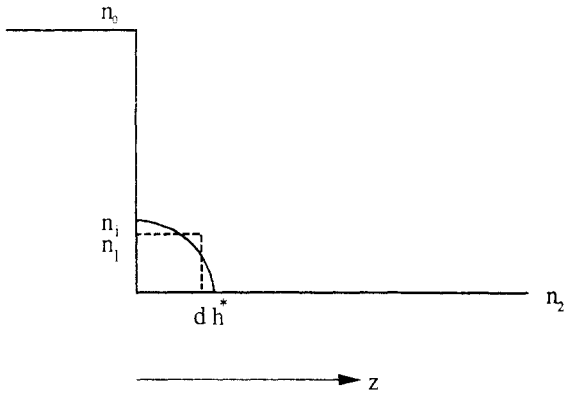

Figure 8. Schematic of the step and parabolic profiles.

surface while the PS chains extend into solution. Both block copolymers have small anchor groups relative to the size of the tails. Surely, there must be a critical PEO length such that the copolymer behaves more like the polystyrene homopolymer and would not adsorb. However, P83/3470, having a tail that is over 40 times larger than the anchor block, adsorbs appreciably, demonstrating the large driving force for the adsorption of block copolymers in selective solvents. The PEO block adsorbs to shield itself from the nonsolvent conditions and binds to the glass through the SiOH sites and the CO polymer groups. There is no apparent difference between the adsorption behavior of P170/1730 on glass and that on sapphire, demonstrating the similarity between these surfaces and, more importantly, the significance of highly unfavorable PEO–solvent interactions in driving adsorption.

Adsorption of Single Chains and Micelles. The results of Figures 2 and 4 indicate different mechanisms of adsorption above and below the critical micelle concentration for P170/1730. Below the cmc, we only have single isolated chains in solution, and therefore adsorption must only occur with individual chains coming to the surface. The fact that the initial rate of adsorption increases with the overall copolymer concentration above the cmc suggests the adsorption of micelles. Above the cmc, there is a constant concentration of single chains in solution. Therefore, if adsorption occurred from single chains alone, the initial rate of adsorption would not change as we increase the overall concentration past the cmc. The ratio of the slopes of the lines in Figure 4 are in qualitative agreement with predictions from the Lévêque solution for transport-limited adsorption for single chains and micelles. More importantly, the 1/3 dependence of the initial adsorption rates on the wall shear rate demonstrates that the adsorption is transport-limited above and below the cmc for the flow rates studied here. Higher flow rates are required to reach kinetic limited adsorption and cannot be achieved with the current flow cell.

Adsorption of single chains appears to result in a more homogeneous coverage of the surface as evidenced by the higher final adsorbed amounts below the cmc than above. Adsorption of micelles, if not accompanied by substantial rearrangement, would lead to a "patchy" surface coverage. When the surface concentration of copolymer chains is estimated on the basis of a random parking of micelles having a radius of 35 nm obtained from dynamic light scattering and an estimate of 50 chains per micelle, the final surface concentration is 2 mg/m^2, within the range of final surface concentrations measured. Since we find that the PS homopolymer does not adsorb, the micelles may adsorb through a rearrangement of its chains, such as an unfolding of the micelle such that the PEO chains will contact the surface. It is also possible that the micelle adsorbs with the polystyrene chains screening the attraction between the PEO blocks and the surface.

To describe the more homogeneous coverage seen just below the cmc, we calculate the dimensionless surface density, σ, from our model for block copolymer adsorption.[2] For the P170/1730 copolymer we estimate a Flory interaction parameter, $\chi = 1.4$, describing the cyclopentane–PEO interaction on the basis of our measured value of the cmc and our model describing micellization.[18] With a PEO-surface attraction of 4 kT,[19] the number of anchor and tail segments, and a solvent size of 1, we calculate a dimensionless surface density of $\sigma = 0.014$, in close agreement with the values presented in Figure 6b.

Surface Concentration, Layer Thickness, and Refractive Index with Time. Figure 6a shows how the average refractive index and layer thickness develop as the surface concentration grows with time for P170/1730. The thickness evolution resembles the surface concentration evolution while the average refractive index quickly attains its final value. We also calculate the surface density of chains and polymer volume fraction as presented in Figure 6b. As the surface density of the layer increases with time due to the adsorption, i.e., as the chains crowd on the surface, the chains extend away from the surface such that the volume fraction is kept relatively constant. This behavior is similar to de Gennes' description of the "mushroom" and "brush" regimes.[20,21] At early times when the surface density is low, the chains do not overlap and the chains resemble mushrooms. As more chains adsorb, the mushrooms will begin to overlap, pushing the tails out and forming more of a brush. For layers forming in this manner, we would expect to see the layer thicken with time with the volume fraction remaining relatively constant. This is in contrast to what would be measured if the coverage grew from islands of chains, i.e., in a patchwise growth. Within an island, the chains would be densely packed, and the solvated tails would be stretched. The surface coverage would develop by growth from the edges of the islands. Since we analyze the results in terms of an equivalent homogeneous film, we would see both the average thickness and volume fraction, or refractive index, increase with time, as the islands cover the surface. However, our results show that only the thickness increases while the volume fraction is constant, showing that the tails stretch as the layer develops. Our results give the first evidence for the mushroom to brush mechanism in the formation of diblock copolymer layers with time.

Our observations of the evolution of the surface concentration and thickness for block copolymers contrast with those of homopolymer polystyrene adsorption on chrome from cyclohexane at the Θ condition.[22-24] For homopolymers, the film thickness establishes very rapidly, while the surface concentration rises slowly. Therefore, after the initial jump in thickness, the volume fraction of the layer increases at constant thickness.

We see that the P170/1730 sample reaches a final layer thickness of 340 Å, over 3.5 times the hydrodynamic radius obtained from dynamic light scattering, and thus the polystyrene chains are moderately stretched. The final surface density of 0.018 is about 5 times the surface density of the chains if they were to occupy an area determined by the hydrodynamic radius of individual coils. Therefore, the P170/1730 copolymer forms a highly compact adsorbed layer that stretches the polystyrene chains. We find in Figure 7a that the P84/3470 copolymer develops an adsorbed layer in the same manner as the P170/1730

copolymer. Again, the layer thickens and the refractive index remains constant as the surface is covered. The layer reaches a thickness of 510 Å, 1.5 times that of the P170/1730 sample.

All theoretical modeling of adsorbed block copolymers in selective solvents predict an extended outer layer. Patel et al.[4] model block copolymers applying the scaling approach developed by Alexander[25] and de Gennes[21] to describe terminally attached polymer chains. At high surface densities, they predict that the layer thickness scales linearly with the molecular weight, $d \sim aN\sigma^{1/3}$, where the surface density, σ, is solely determined by the size of the anchor block. This scaling is also found in the self-consistent-field method of Milner et al.[26] for chains grafted at a fixed surface density. This constant surface density picture applies to some systems with large anchoring blocks; however, when the anchor group is small compared to the tail, the repulsion between tails may govern their surface density.[5] In this case a more complete analysis is required. Equilibrium models, where the surface density is determined in the analysis, show that, in general, the surface density is governed by the repulsion between the solvated tails as well as the packing of the anchor block. Therefore, when the anchor block is small compared to the tail, repulsions between the tails cause the surface density to decrease as the degree of polymerization of the tail increases.[2,3] This leads to a nonlinear scaling easily seen in the geometrical expression for the solvated layer

$$d = aN\sigma/\phi \tag{7}$$

If the surface density, σ, decreases as N increases, the layer thickness has a weaker scaling on N; in fact, no general scaling can be found since the thickness depends on both N and the composition.

Comparing our two samples, we find that the layer thickness depends on the polystyrene degree of polymerization as $d \sim N^{0.58\pm0.03}$, a much weaker dependence than the linear scaling predicted from the models where the anchor groups determine the surface density. This nonlinear scaling is also observed in recent work using a surface-force apparatus; Ansarifar and Luckham[6] have found a relation of $d \sim N^{0.7}$ for block copolymers having small anchor blocks and large tails in good solvent conditions for the tails. In the extreme case of a small anchoring block of one unit, Taunton et al.[8] have also found a nonlinear relationship of $d \sim N^{0.60}$ for a system, denoted PS–X, of polystyrene end-functionalized with a zwitterionic group in a good solvent for polystyrene. These recent experimental results clearly indicate that when the tails are much larger than the anchoring heads, the surface density, σ, decreases as the size of the tail increases due to repulsions between the tails, leading to a weaker dependence on N. It is clear from eq 7 that for constant σ/ϕ one indeed gets $d \sim N$. The larger the tail, the lower the surface density, resulting in a lower scaling exponent. In our mean-field model for block copolymer adsorption, we find $d \sim N^{0.6}$ for small head groups and large tails in a good solvent. The copolymers in our study also have very small anchor blocks with the ratios N_{PEO}/N_{PS} = 0.098 and 0.024, and therefore the scaling exponent is close to 0.6. The fact that the polystyrene chains are in a solvent just above Θ conditions may explain the exponent being slightly below 0.6. Although we have a thicker layer for P83/3470, the layer is more diffuse with a volume fraction constant at ϕ = 0.24 compared to ϕ = 0.46 for P170/1730. We see in Figure 7b that the P83/3470 copolymer, with a tail 40 times larger than the anchor group cannot adsorb at surface densities as high as the P170/1730 copolymer. The mean distance between attachment points given by, $s = a/\sigma^{1/2}$, is 42 Å for P170/1730 and 76 Å for P83/3470. The mean spacings between these copolymers are about half those of the PS–X of Taunton et al.[8] having similar molecular weight for the polystyrene tail. Their polymers were in a better solvent for polystyrene than in our experiments, and therefore it is expected that the mean distance between chains would be greater. In summary, increasing the size of the tails creates a thicker layer but causes the chains to spread laterally to a lower surface density.

Conclusions

We present results on the kinetics of block copolymer adsorption on two dielectric surfaces demonstrating the drastic effect of the overall copolymer concentration. We show that the micellization of block copolymers greatly affects the adsorption. Our results indicate the adsorption of micelles above the cmc, most likely involving rearrangement such that the PEO chains contact the surface. Below the cmc, the adsorption of single chains results in a more homogeneous coverage.

We present the first results showing the time evolution of the surface concentration, thickness, and refractive index of adsorbing block copolymers. Measuring the kinetics of the adsorption provides information on the mechanism of the layer formation. These results indicate the first evidence that, in the formation of an adsorbed layer, block copolymers adsorb like mushrooms, with the tails taking up less space as the surface density increases and eventually forming a high density brush. We see from experiments on two copolymer samples, each having small anchor blocks and large tails, that as the size of the tail becomes larger the surface density of the adsorbed layer decreases, and therefore the thickness shows a weaker than linear dependence on molecular weight, demonstrating the importance of the equilibrium models for block copolymer adsorption.

Acknowledgment. We gratefully acknowledge the support of the Procter & Gamble Corp. through their UERP program, the donors of the Petroleum Research Fund, administered by the American Chemical Society, and the support of Du Pont Marshall Laboratories. M.R.M. was supported by an IBM Graduate Fellowship during the initiation of this work. We thank Jacob Klein and John L. Anderson for providing us with preprints of their work.

Appendix A

The average refractive index and thickness reported here pertain to the step profile of a homogeneous layer as traditionally assumed in optical studies of polymer adsorption. The step profile may be a good approximation to the highly extended layers formed by block copolymers; however, recent work indicates that a parabolic profile[26-28] shown in the schematic of Figure 8

$$n_1(z) = n_i - (n_i - n_2)\left(\frac{z}{h^*}\right)^2 \qquad z < h^*$$

$$n_1(z) = n_2 \qquad z > h^* \tag{A.1}$$

may be more appropriate. Here n_i is the index at the interface, $z = 0$, and h^* is the extent of the layer where $n_1(z)$ equals n_2. To relate the average refractive index, n_1, and thickness, d, of the step profile to n_i and h^* of the parabolic profile, we follow the work of McCrackin and Colson[29] and Stromberg et al.[30] in which the homo-

geneous index n_1 is given by

$$n_1 = \frac{\int_0^\infty n_1(z)(n_1(z) - n_2)\,dz}{\int_0^\infty (n_1(z) - n_2)\,dz} \quad (A.2)$$

where the index profile is a segment density or distribution function. The expression for the average thickness is obtained from eq A.2 and

$$\int_0^\infty (n_1(z) - n_2)\,dz = (n_1 - n_2)d \quad (A.3)$$

to be

$$d = \frac{(\int_0^\infty (n_1(z) - n_2)\,dz)^2}{\int_0^\infty (n_1(z) - n_2)^2\,dz} \quad (A.4)$$

Substituting eq A.1 into eqs A.2 and A.4, we find $n_1 = (4n_i + n_2)/5$ and $d = (5/6)h^*$. Therefore, the parabolic profile thickness would be 1.2 times the thicknesses in Figures 6a and 7a.

Charmet and de Gennes[31] give a different expression for the average or effective thickness as

$$d = \frac{2\int_0^\infty (n_1(z) - n_2)z\,dz}{\int_0^\infty (n_1(z) - n_2)\,dz} \quad (A.5)$$

which gives $d = (3/4)h^*$. Thus, the thicknesses of Figures 6a and 7a are to be multiplied by 1.33 for a parabolic profile following eq A.5. The difference between using the factor of 1.2 or 1.33 from either analysis is within the experimental error in this study. Obviously, the scaling we see is not affected by this factor. Using an average value, we find the P170/1730 extends to about 430 Å and P83/3470 extends to about 650 Å. Taunton et al.[7] have measured an effective layer thickness of 750 Å for the same polymer, P170/1730, in toluene, a good solvent for both PEO and PS. The difference in solvency may explain the difference in the thicknesses.

References and Notes

(1) van Lent, B.; Scheutjens, J. M. H. M. *Macromolecules* **1989**, *22*, 1931.
(2) Munch, M. R.; Gast, A. P. *Macromolecules* **1988**, *21*, 1366.
(3) Evers, O. A.; Scheutjens, J. M. H. M.; Fleer, G. J. *J. Chem. Soc., Faraday Trans. 1*, in press.
(4) Patel, S.; Tirrell, M.; Hadziioannou, G. *Colloids Surf.* **1988**, *31*, 157.
(5) Munch, M. R.; Gast, A. P. *Polym. Commun.* **1989**, *30*, 324.
(6) Ansarifar, M. A.; Luckham, P. F. *Polymer* **1988**, *29*, 329.
(7) Taunton, H. J.; Toprakcioglu, C.; Klein, J. *Macromolecules* **1988**, *21*, 3336.
(8) Taunton, H. J.; Toprakcioglu, C.; Fetters, L. J.; Klein, J. *Nature* **1988**, *332*, 712; Polymers in Regions of Restricted Geometry. *Proceedings of the 197th National Meeting of* the *American Chemical Society*, Dallas, TX, April 9–14, 1989; American Chemical Society: Washington, DC, 1989; p 18.
(9) Webber, R. M.; Anderson, J. L.; Jhon, M. S. *Macromolecules* **1989**, *23*, 1026.
(10) Munch, M. R.; Gast, A. P. *J. Chem. Soc., Faraday Trans. 1*, in press.
(11) Hager, B. L.; Berry, G. C.; Tsai, H.-H. *J. Polym. Sci. B* **1987**, *25*, 387.
(12) Born, M.; Wolf, E. *Principles of Optics*; Pergamon Press: Oxford, 1975.
(13) Tassin, J. F.; Siemens, R. L.; Tang, W. T.; Hadziioannou, G.; Swalen, J. D.; Smith, B. A. IBM Research Report RJ6252 61649, 1988.
(14) Lok, B. K.; Cheng, Y.-L.; Robertson, C. R. *J. Colloid Interface Sci.* **1983**, *91*, 104.
(15) Lévêque, M. *Ann. Mines.* **1928**, *13*, 284.
(16) Brandrup, J., Immergut, E. H., Eds. *Polymer Handbook*; Wiley: New York, 1975.
(17) Mays, J. W.; Ferry, W. M.; Hadjichristidis, N.; Funk, W. G.; Fetters, L. J. *Polymer* **1986**, *27*, 129.
(18) Munch, M. R.; Gast, A. P. *Macromolecules* **1988**, *21*, 1360.
(19) Stuart, M. A. C.; Fleer, G. J.; Scheutjens, J. M. H. M. *J. Colloid Interface Sci.* **1984**, *97*, 526.
(20) de Gennes, P.-G. *Adv. Colloid Interface Sci.* **1987**, *27*, 189.
(21) de Gennes, P.-G. *Macromolecules* **1980**, *13*, 1069.
(22) Takahashi, A.; Kawaguchi, M.; Hirota, H.; Kato, T. *Macromolecules* **1980**, *13*, 884.
(23) Lee, J.-J.; Fuller, G. G. *Macromolecules* **1984**, *17*, 375.
(24) Lee, J.-J. Ph.D. Thesis, Stanford University, 1984.
(25) Alexander, S. *J. Phys.* **1977**, *38*, 983.
(26) Milner, S. T.; Witten, T. A.; Cates, M. E. *Macromolecules* **1988**, *21*, 2610.
(27) Hirz, S. Modeling of Interactions between Adsorbed Block Copolymers. M.S. Thesis, University of Minnesota, 1986.
(28) Cosgrove, T.; Crowley, T. L.; Vincent, B.; Barnett, K. G.; Tadros, T. F. *Faraday Symp. Chem. Soc.* **1981**, *16*, 101.
(29) McCrackin, F. L.; Colson, J. P. In *Ellipsometry in the Measurement of Surfaces and Thin Films*; Passaglia, E., Stromberg, R. R., Kruger, J., Eds.; National Bureau of Standards Symposium: Washington, DC, 1963; p 61.
(30) Stromberg, R. R.; Tutas, D. J.; Passaglia, E. *J. Phys. Chem.* **1965**, *69*, 3955.
(31) Charmet, J. C.; de Gennes, P.-G. *J. Opt. Soc. Am.* **1983**, *73*, 1777.